Inorganic gels as precursors of TiO_2 photocatalysts prepared by low temperature microwave or thermal treatment

Maurizio Addamo [a,*], Marianna Bellardita [a], Daniel Carriazo [b], Agatino Di Paola [a], Stefania Milioto [c], Leonardo Palmisano [a], Vicente Rives [b]

[a] "Schiavello-Grillone" Photocatalysis Group, Dipartimento di Ingegneria Chimica dei Processi e dei Materiali, Università di Palermo, Viale delle Scienze, 90128 Palermo, Italy
[b] Departamento de Química Inorgánica, Universidad de Salamanca, Plaza de la Merced s/n, 37008 Salamanca, Spain
[c] Dipartimento di Chimica Fisica "Filippo Accascina", Università di Palermo, Viale delle Scienze, 90128 Palermo, Italy

ABSTRACT

A simple procedure for preparing active TiO_2 photocatalysts is presented. The starting materials were unusual TiO_2 gels formed from $TiCl_4$. The use of microwaves for a very short time enhanced the TiO_2 crystallinity preventing an increase of particle size and minimizing the decrease of specific surface area. This result makes this preparation very attractive. The formation of the gels was monitored through measurements of viscosity. All the samples were characterized by means of X-ray diffraction, diffuse reflectance spectroscopy and BET specific surface area measurements. The photoactivity of the samples was evaluated using the photodegradation of 4-nitrophenol in liquid–solid regimen and gaseous 2-propanol as probe reactions. Commercial TiO_2 Degussa P25 was used for the sake of comparison.

© 2008 Elsevier B.V. All rights reserved.

1. Introduction

Heterogeneous photocatalysis has been found effective to achieve the photooxidation of many organic pollutants [1–4] and drugs [5,6] present in liquid effluents or in air as volatile organic compounds (VOCs) [7,8]. The most used photocatalyst is TiO_2 due to its (photo)stability, non-toxicity and low cost [9]. TiO_2 exists in three crystalline forms: anatase, brookite and rutile. Anatase is generally accepted to be the most active phase while rutile is the thermodynamically stable form. Pure brookite is very difficult to be prepared and it is often obtained together with the other polymorphic phases [10–13].

TiO_2 photocatalysts are mostly employed as powders but many reports deal with the use of thin films onto various types of supports [14–18]. The sol–gel process is largely used to obtain colloidal solutions, powders or gels. The properties of the samples are strongly dependent not only on the composition but also on the preparation conditions including the starting materials and solvents, the solution preparation sequence and various other experimental conditions as for instance [precursor]/[solvent] ratio, temperature, stirring and aging time [19–21].

Gels are interesting materials because they have high specific surface area (SSA) and are more stable than the corresponding dispersions. Nevertheless, these materials are amorphous or not well crystallized and, consequently, they must be subjected to a suitable treatment to obtain active photocatalysts.

The gels are usually prepared from an alkoxide precursor [22–25] while those obtained by inorganic precursors are not numerous [26,27] although they are more attractive due to the absence of residual amounts of species deriving from the organic moiety. Recently, TiO_2 gels have been prepared by dialysing aqueous solutions obtained by hydrolysis of $TiCl_4$ [19].

The methods used to prepare TiO_2 significantly influence several properties of the photocatalysts that can be related to the observed photoactivity [28,29]. Among the properties, a great importance can be ascribed to crystallinity, SSA and particle size.

An enhancement of crystallinity can be obtained by thermal treatment but the temperature must be carefully selected. By increasing the temperature, the poorly crystalline oxide prepared at low temperature progressively crystallizes to anatase, the active phase, but subsequently it irreversibly transforms into the scarcely active rutile phase [30–32]. The temperature of phase transition depends on the starting materials and on the preparation method. An increase of temperature causes the increase of the mean particle size and the contemporary decrease of SSA, thus negatively influencing the photoactivity of the catalyst [19,30].

---

* Corresponding author.
  E-mail address: addamo@dicpm.unipa.it (M. Addamo).

Catalysts with good properties in terms of crystallinity, SSA and particle size can be prepared by hydrothermal treatment using microwaves as source of energy. Microwave processing of bulk ceramics reduces temperature and time requested for the synthesis, restricting the extent to which particle growth occurs; moreover, very rapid heating rates can be achieved [33–36]. Microwave irradiation furnishes energy to the reactants by means of molecular interaction with the electromagnetic field [37]: the rapid and uniform generation of heat allows the achievement of equilibrium between the bulk and the surface of the material more quickly than with conventional thermal treatment [38].

In recent years several studies have reported on the preparation of TiO_2 powders and films by microwave hydrothermal processing [38–45]. Highly crystalline TiO_2 colloids were obtained by microwave heating colloidal TiO_2 suspensions [46,47] but very little literature on the microwave processing of TiO_2 gels and on the application of microwave heating TiO_2 at relatively low temperatures is available.

In this work, TiO_2 gels were prepared by dialysis of aqueous $TiCl_4$ solutions. The gels were then thermically treated by using either a conventional approach or a microwave hydrothermal treatment. Bulk and surface characterizations of the samples were carried out by means of X-ray diffractometry (XRD), determination of BET specific surface areas and diffuse reflectance spectroscopy (DRS).

4-Nitrophenol (4-NP) photodegradation was selected as a probe reaction to evaluate the photocatalytic efficiency of the various samples. The most active catalysts were also tested for the photodegradation of gaseous 2-propanol. Commercial Degussa P25 was used as a reference photocatalyst.

2. Experimental

2.1. Materials

Titanium tetrachloride (98% Fluka), 4-nitrophenol (>99% Fluka) and 2-propanol (99.8% Fluka) were used without further purification. Titanium dioxide Degussa P25 (anatase and rutile in the ratio 4:1, specific surface area 50 $m^2 g^{-1}$) was utilized as provided.

2.2. Preparation of the samples

The gels were prepared according to a previously published procedure [19] using titanium tetrachloride as the starting material. $TiCl_4$ was slowly added to distilled water ($TiCl_4$:H_2O (v/v) ratio 1:1 or 1:10) and a milky-white dispersion was obtained. After continuous stirring for times ranging between 30 min and 10 h, depending on the initial amount of H_2O, the mixtures became transparent.

These solutions, or those obtained from dilution with water until the $TiCl_4$:H_2O (v/v) ratio of 1:50 or 1:100 was reached [19], were dialysed (dialysis tubing cellulose membrane with MW 12,400 cut-off pores) against water that was replaced every hour. The solutions gradually turned into transparent gels with the exception of the most dilute sample ($TiCl_4$:H_2O (v/v) ratio = 1:100).

The gel formation was followed by measuring the viscosity during the dialysis process by means of a Bohlin Visco 88 viscometer. A spinning cylinder was immersed in the starting solution and the force required to rotate the cylinder at a set speed ($1004 s^{-1}$ at 298 K) was determined as a function of time.

The samples were named G(298, 1 or 10 or 50) where G indicates the gel, 298 the drying temperature and 1, 10 or 50 the $TiCl_4$:H_2O (v/v) ratio. The gels were dried at room temperature under vacuum before their characterization.

Aliquots of gels were calcined in a muffle for 12 h at different temperatures in the range 393–873 K; the resulting samples were named G(T, 1 or 10 or 50) where T indicates the temperature of calcination. Similar amounts of gels were subjected to a microwave treatment for different times at 393 or 423 K in a Milestone Microwave laboratory system, Ethos Plus, High Performance Microwave Lab station. The samples were placed in Teflon vessels and the temperature was increased with a heating rate of 20 °C/min. These samples were named GM(T, t, 1 or 10 or 50) where M indicates the microwave process whereas T and t indicate temperature (K) and duration (min) of the treatment, respectively.

The reproducibility of the synthesis of all samples was tested several times.

2.3. Sample characterization

X-ray diffraction patterns of the powders were recorded at room temperature by a Philips powder diffractometer using the Cu Kα radiation and a 2θ scan rate of $2° min^{-1}$. The diffractograms were used to identify the crystal phase and to evaluate the particle sizes by means of the Scherrer equation. The specific surface areas were determined in a Flow Sorb 2300 apparatus (Micromeritics) by using the single-point BET method. Visible–ultraviolet spectra were obtained by diffuse reflectance spectroscopy by using a Shimadzu UV-2401 PC instrument. $BaSO_4$ was the reference sample and the spectra were recorded in the range 200–600 nm.

2.4. Photoreactivity experiments

The photodegradation of 4-nitrophenol ($C_0 = 20 mg l^{-1}$) was performed in a cylindrical Pyrex batch photoreactor containing 500 ml of aqueous suspension. The reactor was provided with ports in its upper section for the inlet and outlet of gases, for sampling and for pH and temperature measurements. A 125 W medium-pressure Hg lamp (Helios Italquartz, Italy) was immersed within the photoreactor. The photon flux emitted by the lamp was measured by means of a UVX Digital radiometer leaned against the external wall of the photoreactor containing pure water. Under these conditions the emitted flux was 13.5 mW cm^{-2}.

The amount of catalyst was selected by measuring the volume of gel dispersed into the reactor filled with water that was sufficient to absorb all the photons emitted by the lamp. The corresponding TiO_2 content was determined by weighing the solid obtained by drying an equal volume of gel. This method allowed to compare the initial reaction rates of the various samples. The photoreactivity runs were carried out by dispersing the samples (gels or powders) containing 500 mg of TiO_2 in 400 ml of water and adding 100 ml of an aqueous solution of 4-NP ($100 mg l^{-1}$). Oxygen was continuously bubbled through the suspension for 0.5 h before switching on the lamp and throughout the photoreactivity tests. 5 ml of solution was withdrawn at fixed times and the catalyst was separated from the solution through 0.1 μm Teflon membranes (Whatman). 4-Nitrophenol concentration was determined by measuring its absorption at 315 nm with a Shimadzu UV-2401 PC spectrophotometer.

The photodegradation of gaseous 2-propanol was carried out in a cylindrical Pyrex batch reactor ($V = 0.9 l$). The gels were spread on Pyrex glass plates using a simple doctor blade technique. Thin layers of G(773, 10) or Degussa P25 were prepared by spreading the slurries obtained by mixing the powders with water on glass supports that were subsequently dried at 323 K for 30 min.

The samples were placed inside the photoreactor and were irradiated from the top using a 500 W medium-pressure Hg lamp. The irradiance onto the surface of the films was 1.3 mW cm^{-2}. A water filter was interposed between the lamp and the reactor to cut the infrared radiation. The reactor was saturated with O_2 and successively 1 μl of 2-propanol was introduced into the vessel. The

initial concentration of 2-propanol was 15 µM. Samples of 500 µl were withdrawn at fixed intervals using a gas tight syringe. 2-Propanol and propanone concentrations were determined by means of a GC Shimadzu 17A equipped with a HP-1 column and a FID detector, using He as the carrier gas. The amount of CO_2 developed during the photodegradation was followed by using a HP 6890 equipped with a Supelco Carboxen^{TM} column.

3. Results and discussion

Hydrogels are produced when solutions obtained by hydrolysis of $TiCl_4$ in water are dialysed [19,27]. H^+ and Cl^- ions permeate through the membrane and the increasing pH of the retentate is accompanied by the gelation of the solution. The time necessary to form the gel is a function of the initial concentration of $TiCl_4$. When the latter is high enough, the hydrolysis nuclei are numerous so that some of them easily coalesce; if the concentration of $TiCl_4$ is low, the number and size of polymer molecules are too small to form a gel [27].

The formation of hydrogels is accompanied by a large increase of viscosity that is a measure of the resistance to flow of the system due to the layers of molecules which slide over each other. A direct measurement of the viscosity during the dialysis allowed to monitor the formation of the gel [48]. Fig. 1 shows the trend of the viscosity of a 1:10 solution versus time. After a slow progressive increase, the viscosity rapidly rised and reached a maximum. The subsequent decrease was due to the detachment of the gel from the spinning cylinder that prevented to continue the experiment. The formation of gel occurred in the range of pH of the permeate between 2.5 and 3.5. The maximum value of viscosity corresponded to an increase of one order of magnitude with respect to the value of the starting solution. A similar behaviour was noticed when the gel was formed starting from solutions with 1:1 or 1:50 $TiCl_4$:H_2O (v/v) ratios, while for lower ratios no gel formation was observed.

3.1. Structural characterization

Fig. 2 shows the X-ray diffraction patterns of different samples obtained from a solution with a $TiCl_4$:H_2O 1:10 (v/v) ratio. No peaks were observed in the diffractogram of the gel dried at room temperature in agreement with the results of Tanaka and Suganuma [30] who obtained an amorphous gel by hydrolysis of titanium tetrabutoxide at 293 K. The peaks of the anatase phase were detected when the gel was treated in the muffle at 393, 673 and 773 K for 12 h. The crystallinity improved with temperature and the most crystalline sample was obtained at 773 K. The sample G(873, 10) showed the presence of rutile as the main phase. The X-ray patterns of the corresponding samples
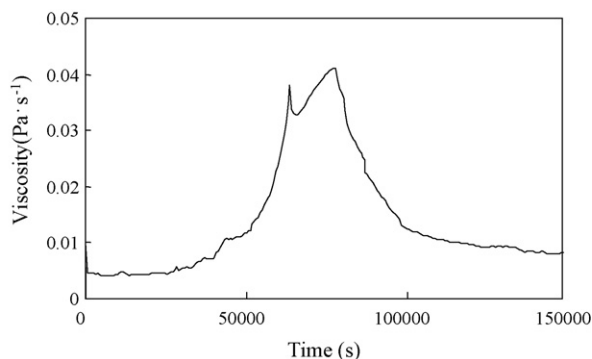

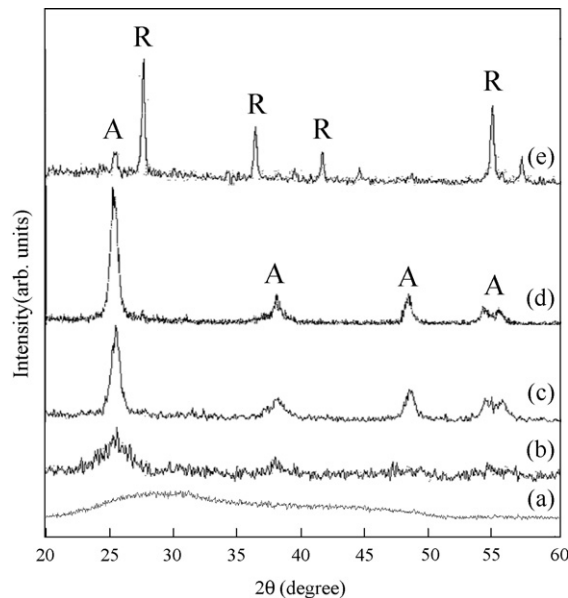**Fig. 1.** Variation of viscosity as a function of time.

Fig. 2. XRD patterns of samples obtained from a solution with a $TiCl_4$:H_2O 1:10 (v/v) ratio: (a) G(298, 10); (b) G(393, 10); (c) G(673, 10); (d) G(773, 10); and (e) G(873, 10).

obtained from solutions with different $TiCl_4$:H_2O ratios were similar to those shown in Fig. 2

The crystallite sizes determined by the Scherrer equation are reported in Table 1. The anatase crystallite size slightly increased up to 673 K while at 873 K it reached the maximum value, indicating the grain coarsening induced by the heating treatment. The transformation from anatase to rutile occurred in the range 773–873 K. A transition temperature above 873 K is reported for a calcined gel obtained from an organic precursor [30] but it is known that the polymorphic phase transformation is influenced by the method of synthesis of the parent TiO_2 oxide [31].

Interestingly, microwave treatment allowed to obtain quite crystalline samples without increase of the particle size that is opposite to what usually observed in the conventional heating treatment in the muffle. Fig. 3 shows X-ray patterns of samples obtained from solutions with different $TiCl_4$:H_2O ratios treated in the microwave oven at 393 K for 30 min. The crystallinity of the various samples was higher than that obtained with a treatment of 12 h in the muffle at the same temperature. The most crystalline sample was obtained from the solution with the lowest $TiCl_4$ concentration. It is worth noting that the XRD patterns of samples subjected to thermal treatment in muffle for 30 min at the same temperature did not reveal crystalline peaks.

No significant enhancement of crystallinity was observed when the microwave treatment time was extended to 1 h. This finding agrees with the results of previous works reporting that an extremely rapid crystallization occurs under microwave irradiation. Murugan et al. [43] obtained nanocrystalline anatase phase in very short times by microwave hydrothermal treatment. Crystallization of rutile from $TiOCl_2$ solutions was also found to be very fast [39]. This phenomenon can be probably explained by invoking high temperatures domains generated by microwaves.

The gel obtained from the solution with the 1:10 $TiCl_4$:H_2O (v/v) ratio was treated at 423 K for 15 and 30 min. 423 K was the maximum temperature value feasible in our microwave apparatus since higher temperatures caused an increase of pressure incompatible with the Teflon vessel used. The XRD patterns reported in Fig. 4 reveal that anatase was the only crystallographic phase. The comparison with commercial Degussa P25 shows that

Table 1
Treatments, crystalline phases ([A] = anatase; [R] = rutile) and particles size (Φ) of the various samples

| Sample	Treatment	Phase	Φ (nm)
G(298, 1)	Gel 1:1 dried at 298 K	Amorphous	–
G(298, 10)	Gel 1:10 dried at 298 K	Amorphous	–
G(298, 50)	Gel 1:50 dried at 298 K	Amorphous	–
G(393, 1)	Gel 1:1 calcined in muffle at 393 K for 12 h	A	25 [A]
G(673, 1)	Gel 1:1 calcined in muffle at 673 K for 12 h	A	28 [A]
G(773, 1)	Gel 1:1 calcined in muffle at 773 K for 12 h	A	38 [A]
G(873, 1)	Gel 1:1 calcined in muffle at 873 K for 12 h	A (10%) – R (90%)	40 [A], 90 [R]
G(393, 10)	Gel 1:10 calcined in muffle at 393 K for 12 h	A	20 [A]
G(673, 10)	Gel 1:10 calcined in muffle at 673 K for 12 h	A	23 [A]
G(773, 10)	Gel 1:10 calcined in muffle at 773 K for 12 h	A	30 [A]
G(873, 10)	Gel 1:10 calcined in muffle at 873 K for 12 h	A (9%) – R (91%)	35 [A], 80 [R]
G(393, 50)	Gel 1:50 calcined in muffle at 393 K for 12 h	A	18 [A]
G(673, 50)	Gel 1:50 calcined in muffle at 673 K for 12 h	A	22 [A]
G(773, 50)	Gel 1:50 calcined in muffle at 773 K for 12 h	A	29 [A]
G(873, 50)	Gel 1:50 calcined in muffle at 873 K for 12 h	A (10%) – R(90%)	32 [A], 69 [R]
GM(393, 30, 1)	Gel 1:1 treated at 393 K for 30 min with microwave	A	18 [A]
GM(393, 60, 1)	Gel 1:1 treated at 393 K for 60 min with microwave	A	25 [A]
GM(393, 30, 10)	Gel 1:10 treated at 393 K for 30 min with microwave	A	16 [A]
GM(393, 60, 10)	Gel 1:10 treated at 393 K for 60 min with microwave	A	20 [A]
GM(393, 30, 50)	Gel 1:50 treated at 393 K for 30 min with microwave	A	16 [A]
GM(393, 60, 50)	Gel 1:50 treated at 393 K for 60 min with microwave	A	20 [A]
GM(423, 15, 10)	Gel 1:10 treated at 423 K for 15 min with microwave	A	19 [A]
GM(423, 30, 10)	Gel 1:10 treated at 423 K for 30 min with microwave	A	20 [A]
Degussa P25	As-received	A (80%) – R (20%)	25 [A], 33 [R]

the samples were quite crystalline and crystallinity increased with increasing the treatment time. The size of the particles remained very small (see Table 1) and it was scarcely influenced by the increase of temperature from 393 to 423 K.

Table 2 reports some physico-chemical properties of the various samples. The specific surface areas of the gels were quite high and increased with decreasing the $TiCl_4$:H_2O ratio. When the gels were calcined in the muffle at 393 K the surface areas dramatically decreased from values ranging between 230 and 280 $m^2 g^{-1}$ to values between 90 and 120 $m^2 g^{-1}$. The thermal treatment caused an irreversible agglomeration process of the anatase nanocrystallites that increased with the temperature. Very low SSA values (10–13 $m^2 g^{-1}$) were obtained at 873 K due to the presence of rutile as the main phase.

Differently, the microwave treatment did not lead to a considerable decrease of the specific surface areas whose values ranged from 150 to 200 $m^2 g^{-1}$ for the samples treated at 393 K and were equal to 140 $m^2 g^{-1}$ for the samples treated at 423 K. Moreover, it is worth noting that the duration of the treatment did not significantly affect the SSA values.

It can be concluded that the microwave treatment does not induce important effects of agglomeration and this finding is significant from the photocatalytic point of view.

Fig. 5 shows the diffuse reflectance spectra of some samples. By assuming TiO_2 as an indirect semiconductor [49] the band gap energy, E_g, of each sample (see Table 2) has been estimated from the tangent line in the plot of the modified Kubelka–Munk function $[F(R'_\infty)h\nu]^{1/2}$ versus the energy of the exciting light [19,50], as
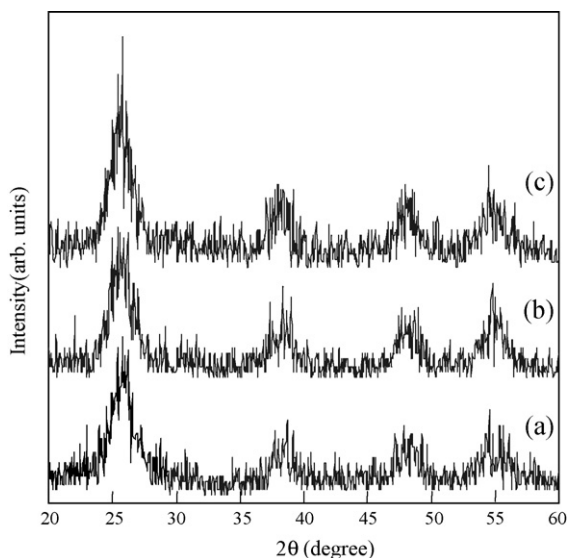
Fig. 3. XRD patterns of samples obtained from solutions with different $TiCl_4$:H_2O ratios, after 30 min of microwave treatment at 393 K: (a) GM(393, 30, 1); (b) GM(393, 30, 10); and (c) GM(393, 30, 50).
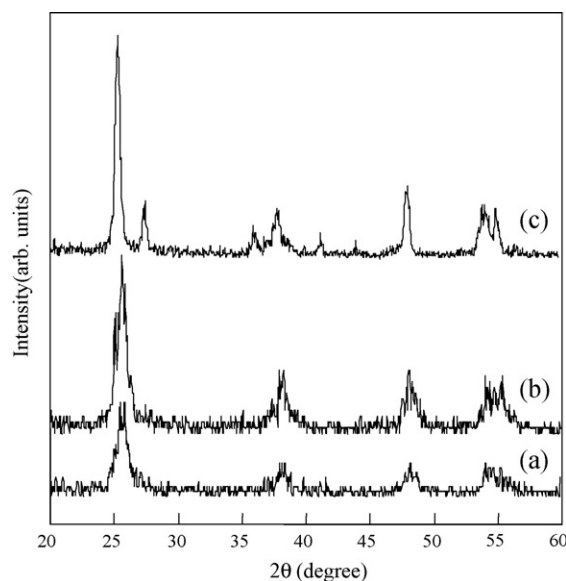
Fig. 4. XRD patterns of selected samples: (a) GM(423, 15, 10); (b) GM(423, 30, 10); and (c) Degussa P25.

Table 2
Specific surface areas (SSAs), initial reaction rates for 4-NP photodegradation (r_0) and band gap values (E_g) of the various samples

Sample	SSA ($m^2 g^{-1}$)	E_g (eV)	r_0 ($\times 10^9$ mol l^{-1} s^{-1})
G(298, 1)	230	3.10	Negligible
G(298, 10)	250	3.10	Negligible
G(298, 50)	280	3.10	Negligible
G(393, 1)	90	3.10	7
G(673, 1)	75	3.14	10
G(773, 1)	60	3.15	15
G(873, 1)	10	3.02	2
G(393, 10)	100	3.11	10
G(673, 10)	90	3.12	15
G(773, 10)	84	3.11	22
G(873, 10)	12	3.03	4
G(393, 50)	120	3.10	8
G(673, 50)	95	3.12	13
G(773, 50)	85	3.13	20
G(873, 50)	13	3.03	2
GM(393, 30, 1)	150	3.08	12
GM(393, 60, 1)	150	3.12	13
GM(393, 30, 10)	180	3.10	33
GM(393, 60, 10)	170	3.13	32
GM(393, 30, 50)	200	3.11	30
GM(393, 60, 50)	180	3.11	31
GM(423, 15, 10)	140	3.15	47
GM(423, 30, 10)	140	3.17	93
Degussa P25	50	3.15	50

shown in the inset of Fig. 5. The band gap values ranged between 3.03 eV (the sample with the highest content of rutile) and 3.17 eV (the sample consisting of the best crystalline anatase). These values are very close to those determined for pure commercial anatase and rutile samples, respectively [13].

3.2. Photocatalytic properties

The disappearance of 4-NP was followed by determining the concentration of the substrate at various time intervals. The photoactivity of the various samples was compared with that of commercial Degussa P25 TiO$_2$. The degradation rate, r_0, was calculated from the initial slope (extrapolated in the first 30 min of the runs) of the concentration versus time profiles. The r_0 values are reported in Table 2.
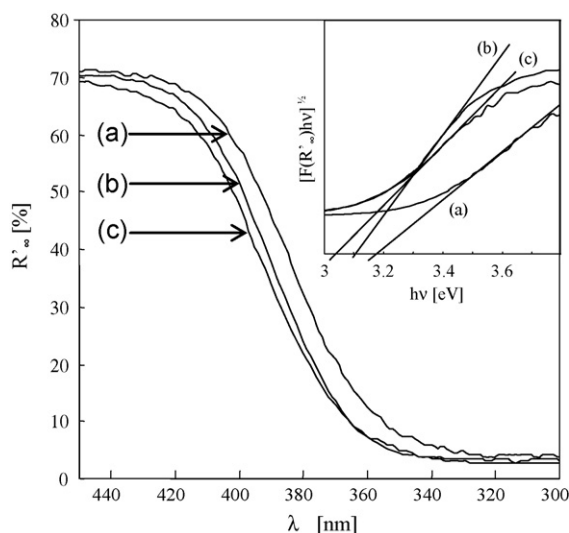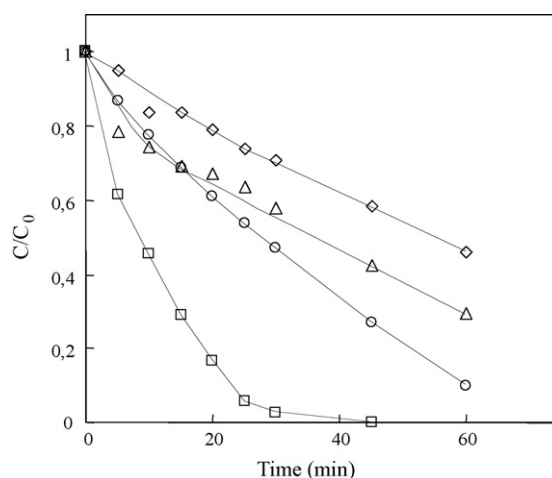
The as-prepared gels revealed a negligible activity. This result is most likely ascribable to the amorphous nature of these samples as resulted from the XRD analysis.

The photoactivity of the gels calcined in the muffle increased with temperature, reaching a maximum value at 773 K that can be attributed to a better crystallization of the anatase phase. At 873 K the photoactivity markedly decreased due to the formation of rutile. The TiCl$_4$:H$_2$O (v/v) ratios did not significantly influence the photoactivity of the samples. In fact, the initial reaction rates obtained with the gels calcined at 773 K were quite similar, ranging between 15 and 22 mol l s^{-1}. The lowest value was found for G(773, 1) and the highest for G(773, 10). These results are not surprising considering that the samples with the highest TiCl$_4$:H$_2$O (v/v) ratio have specific surface areas slightly smaller than those with lower ratios. It is worth noting that the samples with a TiCl$_4$:H$_2$O 1:10 (v/v) ratio were the most photoactive at all calcination temperatures.

The influence of the TiCl$_4$:H$_2$O (v/v) ratio was more relevant when the gels were treated with the microwaves. The initial reaction rates of the samples obtained at 393 K from gels with the lowest TiCl$_4$:H$_2$O ratios, i.e. 1:10 and 1:50, were very similar, whereas the r_0 values of the samples prepared from gels with a TiCl$_4$:H$_2$O 1:1 ratio were about one-third. GM(393, 30, 10) was the most photoactive sample obtained at this temperature.

The gel obtained with the TiCl$_4$:H$_2$O 1:10 ratio was chosen to prepare the GM(423, 15, 10) and GM(423, 30, 10) samples. Runs carried out in the presence of GM(423, 15, 10) revealed a higher initial reaction rate than that measured in the presence of GM(393, 30, 10) that was subjected to a longer duration of microwave treatment but at a lower temperature.

Fig. 6 shows the disappearance of 4-NP as a function of the irradiation time in the presence of some selected samples. The activity of the best photocatalysts prepared by microwave heating was significantly higher than that of the samples calcined in muffle: after 1 h of irradiation, ca. 70% of substrate was degraded in the presence of GM(393, 30, 50) whereas only 55% of 4-NP was transformed with G(773, 10). The sample GM(423, 30, 10) was more efficient than the very active Degussa P25 TiO$_2$: 4-NP was completely degraded within ca. 45 min whereas more than 1.5 h was necessary when P25 was used. This finding can be explained by considering that the microwave treatment produces a high crystallinity of the samples but it does not cause a great increase of the particles size and the corresponding decrease of specific

Fig. 5. Diffuse reflectance spectra of various samples: (a) GM(423, 30, 10); (b) G(773, 10); and (c) G(873, 10). The band gap determination is reported in the inset.

Fig. 6. Disappearance of 4-NP in the presence of different samples: (◇) G(773, 10); (△) GM(393, 30, 50); (□) GM(423, 30, 10); (○) Degussa P25. Initial 4-NP concentration: 0.14 mM.
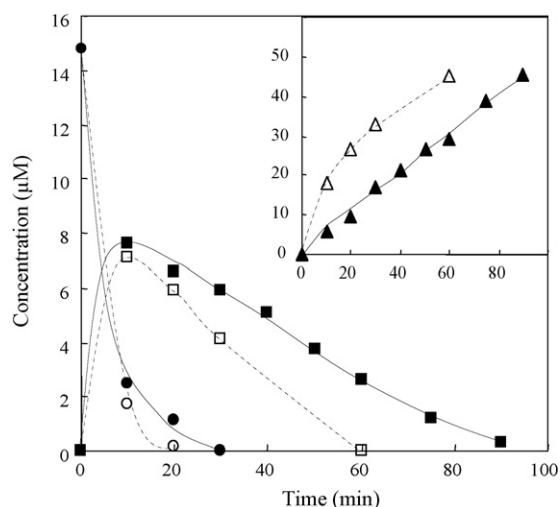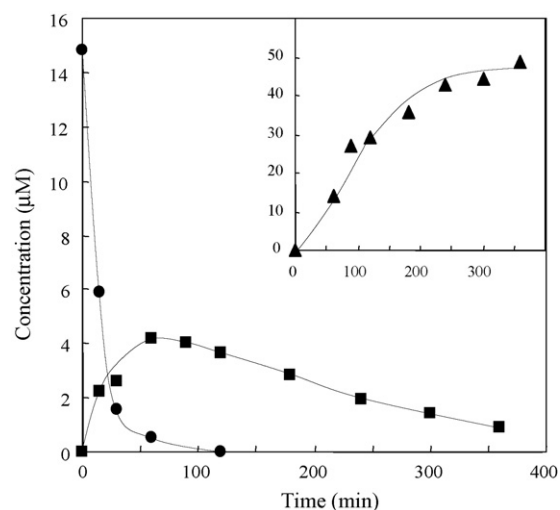
Fig. 7. Changes of 2-propanol (●, ○) and propanone (■, □) concentration in the presence of G(773, 10) (full symbols) and Degussa P25 (open symbols). The inset shows the evolution of CO_2 (▲, □) during the photodegradation. Initial 2-propanol concentration: 15 μM.

surface area. As shown by time resolved microwave photoconductivity (TRMC) measurements [51–53], high crystalline quality leads to long lifetimes of the charge carriers favouring the reaction with the species to be photodegraded [52]. Higher specific surface areas induce higher numbers of accessible active sites and consequently a better reactivity [53].

The most active samples prepared by calcining or microwave treatment were also tested for the photodegradation of gaseous 2-propanol. The main intermediate product was propanone that was further oxidized to CO_2 [54]. Fig. 7 shows the variations of 2-propanol and propanone concentration under UV irradiation in the presence of Degussa P25 and G(773, 10), respectively. The complete disappearance of 2-propanol was reached after about 20 min with Degussa P25 and 30 min by using G(773, 10). Propanone rapidly increased, reached a maximum and then disappeared within 60 min with Degussa P25 and after 90 min with G(773, 10).

As shown in Fig. 8, 120 min was necessary for the complete degradation of 2-propanol in the presence of GM(423, 30, 10).

Fig. 8. Changes of 2-propanol (●) and propanone (■) concentration in the presence of GM(423, 30, 10). The inset shows the evolution of CO_2 during the photodegradation. Initial 2-propanol concentration: 15 M.

Propanone slowly increased until a maximum and began to be degraded only when the concentration of 2-propanol was very low. Propanone completely disappeared within 7 h.

The insets of Figs. 7 and 8 reveal that 2-propanol was always stoichiometrically transformed into CO_2. The measured final concentration of CO_2 was three times the initial concentration of 2-propanol confirming that the substrate was completely mineralized in the presence of the three photocatalysts.

The relatively low activity exhibited by GM(423, 30, 10) in gas–solid regimen can be explained by considering that the presence of a noticeable amount of water in the gel network reduces the relative amount of TiO_2 sites present in the surface of the catalyst. Moreover also a sequestrating effect of water could be considered. The consequence is a formation of propanone slower than that observed in the presence of P25 or G(773, 10).

4. Conclusion

Microwave irradiation at low temperatures has been applied to synthesize active TiO_2 photocatalysts. The starting materials were unusual gels prepared by dialysis of aqueous solutions obtained by hydrolysis of $TiCl_4$.

The powders obtained by calcining the gels in the muffle at high temperatures were less active for the photodegradation of 4-nitrophenol than the corresponding samples prepared by microwave processing.

Short times of microwave heating were sufficient to obtain a good crystallinity at lower temperatures than with the conventional thermal treatment, without significant changes of particle size and reduction of specific surface area.

A highly active sample revealed a photoactivity ca. twice that of commercial TiO_2 Degussa P25 when it was tested in solid–liquid regimen. Instead, a relatively low efficiency for the photooxidation of gaseous 2-propanol was obtained, due to the large amount of water present in the gel that reduces the number of active TiO_2 surface sites.

References

[1] M. Schiavello (Ed.), Heterogeneous Photocatalysis, Wiley, New York, 1995.
[2] D.F. Ollis, H. Al-Ekabi (Eds.), Photocatalytic Purification and Treatment of Water and Air, Elsevier, Amsterdam, 1993.
[3] G. Marcì, M. Addamo, V. Augugliaro, S. Coluccia, E. García-López, V. Loddo, G. Martra, L. Palmisano, M. Schiavello, J. Photochem. Photobiol. A: Chem. 160 (2003) 105–114.
[4] M.R. Hoffmann, T.S. Martin, W. Choi, D.W. Bahnemann, Chem. Rev. 95 (1995) 69–96.
[5] M. Addamo, V. Augugliaro, A. Di Paola, E. García-López, V. Loddo, G. Marcì, L. Palmisano, J. Appl. Electrochem. 35 (2005) 765–774.
[6] A. Di Paola, M. Addamo, V. Augugliaro, E. García-López, V. Loddo, G. Marcì, L. Palmisano, Int. J. Photoenergy 8 (2006) 1–6.
[7] J. Peral, X. Domenech, D.F. Ollis, J. Chem. Technol. Biotechnol. 70 (1997) 117–140.
[8] K. Hashimoto, K. Wasada, N. Toukai, H. Kominami, Y. Kera, J. Photochem. Photobiol. A: Chem. 136 (2000) 103–109.
[9] A. Fujishima, K. Hashimoto, T. Watanabe, TiO$_2$ Photocatalysis: Fundamentals and Applications, BKC, Tokyo, 1999.
[10] Y. Zheng, E. Shi, S. Cui, W. Li, X. Hu, J. Am. Ceram. Soc. 83 (2000) 2634–2636.
[11] A. Pottier, C. Chaneac, E. Tronc, L. Mazarolles, J. Jolivet, J. Mater. Chem. 11 (2001) 1116–1121.
[12] R.C. Bhave, B.I. Lee, Mater. Sci. Eng. A 467 (2007) 146–149.
[13] A. Di Paola, G. Cufalo, M. Addamo, M. Bellardita, R. Campostrini, M. Ischia, R. Ceccato, L. Palmisano, Colloid Surf. A: Physicochem. Eng. Aspects 317 (2008) 366–376.
[14] J. Yu, X. Zhao, Q. Zhao, Thin Solid Films 379 (2000) 7–14.

[15] N. Smirnova, A. Eremenko, O. Rusina, W. Hopp, L. Spanhel, J. Sol–Gel Sci. Technol. 22 (2001) 109–113.
[16] I.M. Arabatzis, S. Antonaraki, T. Stergiopoulos, A. Hiskia, E. Papaconstantinou, M.C. Bernard, P. Falaras, J. Photochem. Photobiol. A: Chem. 149 (2002) 237–245.
[17] M. Addamo, M. Bellardita, A. Di Paola, L. Palmisano, Chem. Commun. (2006) 4943–4945.
[18] A. Di Paola, M. Addamo, M. Bellardita, E. Cazzanelli, L. Palmisano, Thin Solid Films 515 (2007) 3527–3529.
[19] M. Addamo, V. Augugliaro, A. Di Paola, E. García-López, V. Loddo, G. Marcì, L. Palmisano, Colloid Surf. A: Physicochem. Eng. Aspects 265 (2005) 23–31.
[20] M. Anpo, T. Shima, S. Kodama, Y. Kubokawa, J. Phys. Chem. 91 (1987) 4305–4310.
[21] C.J. Brinker, G.W. Scherer, Sol–Gel Science: The Physics and Chemistry of Sol–Gel Processing, Academic Press, New York, 1990.
[22] G. Dagan, M. Tomkiewicz, J. Phys. Chem. 97 (1993) 12651–12655.
[23] P.D. Moran, J.R. Bartlett, G.A. Bowmaker, J.L. Woolfrey, R.P. Cooney, J. Sol–Gel Sci. Technol. 15 (1999) 251–262.
[24] M. Krunks, I. Oja, K. Tonsuaadu, M. Es-Souni, M. Gruselle, L. Niinisto, J. Therm. Anal. Calc. 80 (2005) 483–488.
[25] V. Balek, N. Todorova, C. Trapalis, V. Stengl, E. Vecernikova, J. Subrt, Z. Malek, G. Kordas, J. Therm. Anal. Calc. 80 (2005) 503–509.
[26] J. Moon, H. Takagi, Y. Fujishiro, M. Awano, J. Mater. Sci. 36 (2001) 949–955.
[27] Y. Chen, A. Lin, F. Gan, Powder Technol. 167 (2006) 109–116.
[28] H. Kominami, M. Kohno, Y. Matsunaga, Y. Kera, J. Am. Ceram. Soc. 84 (2001) 1178–1180.
[29] M. Addamo, V. Augugliaro, A. Di Paola, E. García-López, V. Loddo, G. Marcì, R. Molinari, L. Palmisano, M. Schiavello, J. Phys. Chem. B 108 (2004) 3303–3310.
[30] Y. Tanaka, M. Suganuma, J. Sol–Gel Sci. Technol. 22 (2001) 83–89.
[31] S.A. Borkar, S.R. Dharwadkar, Ceram. Int. 30 (2004) 509–514.
[32] S. Cerneaux, X. Xiong, G.P. Simon, Y.-B. Cheng, L. Spiccia, Nanotechnology 18 (2007), 055708.
[33] K.N. Ramakrishnan, Mater. Sci. Eng. A 259 (1999) 120–125.
[34] D.D. Upadhyaya, A. Ghosh, G.K. Dey, R. Prasad, A.K. Suri, J. Mater. Sci. 36 (2001) 4707–4710.

[35] D.K. Agrawal, Curr. Opin. Solid State Mater. Sci. 3 (1998) 480–485.
[36] G.-F. Xu, I.K. Lloyd, Y. Carmel, T. Olorunyolemi, O.C.J. Wilson, J. Mater. Res. 16 (2001) 2850–2858.
[37] L.-X. Zhang, P. Liu, Z.-X. Su, Mater. Res. Bull. 41 (2006) 1631–1637.
[38] J.N. Hart, D. Menzies, Y.-B. Cheng, G.P. Simon, L. Spiccia, Sol. Energy Mater. Sol. Cells 91 (2007) 6–16.
[39] S. Komarneni, R.K. Rajha, H. Katsuki, Mater. Chem. Phys. 61 (1999) 50–54.
[40] J.N. Hart, R. Cervini, Y.-B. Cheng, G.P. Simon, L. Spiccia, Sol. Energy Mater. Sol. Cells 84 (2004) 135–143.
[41] X. Wu, Q.-Z. Jing, Z.-F. Ma, M. Fu, W.-F. Shangguan, Solid State Commun. 136 (2005) 513–517.
[42] A. Bonamartini Corradi, F. Bondioli, B. Focher, A.M. Ferrari, C. Grippo, E. Mariani, C. Villa, J. Am. Ceram. Soc. 88 (2005) 2639–2641.
[43] A.V. Murugan, V. Samuel, V. Ravi, Mater. Lett. 60 (2006) 479–480.
[44] A. Jaroenworaluck, T. Panyathanmaporn, B. Soontornworajit, S. Supothina, Surf. Interf. Anal. 38 (2006) 765–768.
[45] X. Jia, W. He, X. Zhang, H. Zhao, Z. Li, Y. Feng, Nanotechnology 18 (2007) 075602.
[46] G.J. Wilson, G.D. Will, R.L. Frost, S.A. Montgomery, J. Mater. Chem. 12 (2002) 1787–1791.
[47] G.J. Wilson, A.S. Matijasevich, D.R.G. Mitchell, J.C. Schulz, G.D. Will, Langmuir 22 (2006) 2016–2027.
[48] D. Bonn, H. Kellay, H. Tanaka, G. Wegdam, J. Meunier, Langmuir 15 (1999) 7534–7536.
[49] F.P. Koffyberg, K. Dwight, A. Wold, Solid State Commun. 30 (1979) 433–437.
[50] Y.I. Kim, S.J. Atherton, E.S. Brigham, T.E. Mallouk, J. Phys. Chem. 97 (1993) 11802–11810.
[51] K.-M. Schindler, M. Kunst, J. Phys. Chem. 94 (1990) 8222–8226.
[52] C. Colbeau-Justin, M. Kunst, D. Huguenin, J. Mater. Sci. 38 (2003) 2429–2437.
[53] S. Boujday, F. Wünsch, P. Portes, J.F. Bocquet, C. Colbeau-Justin, Sol. Energy Mater. Sol. Cells 83 (2004) 421–433.
[54] Y. Ohko, A. Fujishima, K. Hashimoto, J. Phys. Chem. B 102 (1998) 1724–1729.